Reproducibility of ^{11}C-Raclopride Binding in the Rat Brain Measured with the MicroPET R4: Effects of Scatter Correction and Tracer Specific Activity

David L. Alexoff, BSE[1]; Paul Vaska, PhD[2]; Douglas Marsteller, MS[3]; Timofei Gerasimov[1]; Juan Li, MA[4]; Jean Logan, PhD[1]; Joanna S. Fowler, PhD[1]; Nicholas B. Taintor, MS[2]; Panayotis K. Thanos, PhD[2]; and Nora D. Volkow, MD[2]

[1]Chemistry Department, Brookhaven National Laboratory, Upton, New York; [2]Medical Department, Brookhaven National Laboratory, Upton, New York; [3]Department of Pharmacological Sciences, State University of New York at Stony Brook, Stony Brook, New York; and [4]Department of Applied Mathematics and Statistics, State University of New York at Stony Brook, Stony Brook, Stony Brook, New York

A new generation of commercial animal PET cameras may accelerate drug development by streamlining preclinical testing in laboratory animals. However, little information on the feasibility of using these machines for quantitative PET in small animals is available. Here we investigate the reproducibility of microPET imaging of ^{11}C-raclopride in the rat brain and the effects of tracer-specific activity and photon scatter correction on measures of D2 receptor (D2R) availability. **Methods:** Sprague–Dawley rats (422 ± 29 g; $n = 7$) were anesthetized with ketamine/xylazine and catheterized for tail vein injection of ^{11}C-raclopride. Each animal was positioned prone in the micro-PET, centering the head in the field of view. MicroPET data was collected for 60 min—starting at ^{11}C-raclopride injection—and binned into 24 time frames (6 × 10 s, 3 × 20 s, 8 × 60 s, 4 × 200 s, 3 × 600 s). In 3 studies, ^{11}C-raclopride was administered a second time in the same animal, with 2–4 h between injections. In a fourth animal, raclopride (1 mg/kg) was coinjected with ^{11}C-raclopride for the second injection. Three rats received a single dose of ^{11}C-raclopride. The range of doses for all studies was 6.11–18.54 MBq (165–501 μCi). The specific activity at injection was 4.07–48.1 GBq/μmol (0.11–1.3 Ci/μmol). Region-of-interest analysis was performed and the distribution volume ratio (DVR) was computed for striatum/cerebellum using sinograms uncorrected and corrected for scatter using a tail-fit method. **Results:** Test–retest results showed that the ^{11}C-raclopride microPET DVR was reproducible (change in DVR = −8.3% ± 4.4%). The average DVR from 6 rats injected with high specific activity (<4 nmol/kg) was 2.43 ± 0.19 (coefficient of variation = 8%). The DVR for the blocking study was 1.23. The DVR depended on the mass of tracer ^{11}C-raclopride injected for doses >1.5 nmol/kg. Scatter fractions within the rat head were ~25%–45% resulting in an average increase of DVR of 3.5% (range, 0%–10%) after correction. **Conclusion:** This study shows that the ^{11}C-raclopride microPET–derived DVR is reproducible and suitable for studying D2R availability in the rat brain. MicroPET sensitivity was sufficient to determine reproducible DVRs from ^{11}C-raclopride injections of 9.25 MBq (~250 μCi). However, the effect of tracer mass on the DVR should be considered for studies using more than ~1–2 nmol/kg raclopride, and scatter correction has a measurable impact on the results.

Key Words: microPET; rat brain; dopamine receptor; raclopride

J Nucl Med 2003; 44:815–822

The recent commercialization of a new generation of high-resolution small-animal PET cameras (microPET, Concorde Microsystems, Knoxville, TN; and HIDAC, Oxford Positron Systems, Oxford, U.K.) (*1,2*) is expected to expand the use of PET methods in basic research and new drug development by facilitating in vivo imaging in small animals. PET methodologies based on specially designed, dedicated animal cameras can be used early in new radiopharmaceutial and drug development to measure temporal and spatial distributions of drugs and tracers, to estimate kinetic rate constants, and to evaluate the relationship of receptor occupancy to drug efficacy in vivo (*3–5*). In addition, high-resolution PET can help unify decades of biologic research in laboratory animals with human biology by permitting more direct comparisons of animal research with clinical research (*6*). For example, small-animal PET imaging of the rodent brain has been used to study dopaminergic function in animal models of human brain disorders, including Parkinson's disease (*7*), Huntington's disease (*7–9*), and drug abuse (*10*). These methods have been recently extended to imaging of dopaminergic function in genetically manipulated (D2 receptor [D2R] knockout) mice (*11*). PET imaging of transgenic animals is particularly exciting

because it permits the direct study of the relationship between specific genes and organ function as well as the mechanisms underlying regulation of gene expression (*12*). Finally, in vivo imaging of rodents can be used to characterize the chronic effects of drug treatments using a single animal, thus mimicking long-term drug therapy in humans. For example, PET imaging of the rat brain has been used to help elucidate a neurochemical basis for fluctuations in the efficacy of chronic levodopa treatment of Parkinson's disease (*13*).

The feasibility of using specially designed, dedicated animal PET cameras to study dopaminergic function in the rodent brain was first investigated >5 y ago using a custom-built tomograph with a spatial resolution of 3- to 4-mm full width at half maximum (FWHM) near the center (*7*). This and more recent studies of the rat D2R system (*8,14,15*) have demonstrated that custom-built, high-resolution PET cameras can give reproducible data that are highly correlated with established ex vivo and postmortem techniques. With the appearance of a new generation of commercial animal PET cameras, the need for similar feasibility studies is apparent. Recently, our laboratory acquired the microPET R4 (Concorde Microsystems), a high-resolution tomograph designed especially for rodent imaging. Although a performance evaluation of the microPET P4—the machine identical to the model R4 except with a larger system radius—was recently published (*1*), little information is available on the practical application of commercial microPET to characterizing dopamine receptor function in the rat brain. The goal of this work was to evaluate the application of the microPET R4 to D2R imaging in the rat brain using ^{11}C-raclopride. Specifically, we address the reproducibility of ^{11}C-raclopride binding and determinations of the distribution volume ratio (DVR) used to assess D2R availability. The reproducibility was determined using a test–retest paradigm, thus extending the work of earlier studies that describe primarily the reproducibility of kinetic measurements within a group of rats (*7,13,15–17*). In addition, to address the impact of ~2-mm resolution of modern small-animal PET cameras, we compared measures of binding potential (DVR-1) and striatum/cerebellum (ST/CB) ratios to previously published results using lower resolution machines.

Finally, it was important to validate the quantitative capabilities of the commercial microPET, especially with respect to corrections for photon attenuation and scatter that are not yet functional in the vendor software. Although attenuation correction factors for both the rat striatum and cerebellum have been determined previously (*17*), little information is available on the contribution of scatter to PET measurements in the rat striatum and cerebellum. Hence, for these studies, we focused on the effect of scatter correction on dynamic microPET measurements of ^{11}C-raclopride in the rat brain.

MATERIALS AND METHODS

Animals

Seven adult, male Sprague–Dawley rats (Taconic, Germantown, NY) were anesthetized with ketamine (100 mg/kg) and xylazine (10 mg/kg) and catheterized for lateral tail vein injection of radiotracer. The rats weighed 422 ± 29 g. Rats were individually housed and food and water were provided ad lib. This work was approved by the Institutional Animal Care and Use Committee of Brookhaven National Laboratory, and all rats were housed and maintained in an accredited animal husbandry facility that was approved by the Association for Assessment of Laboratory Animal Care.

[11]C-Raclopride Preparation

[11]C-Raclopride was synthesized according to the method described previously (*18*). ^{11}C-Raclopride doses were small fractions of routine syntheses prepared for human subject studies. Specific activity determination was made using mass measurements acquired during radiotracer purification by high-performance liquid chromatography (HPLC) (Novapak C18, 250 × 10 mm; Waters, Milford, MA) and radioactivity measurements obtained with a calibrated ion chamber (Capintec, Inc., Ramsey, NJ).

PET

Imaging was performed using the microPET R4 tomograph (Concorde Microsystems), which has a 12-cm animal port with an image field of view (FOV) of ~11.5 cm. Three animals received a single injection of ^{11}C-raclopride, whereas 4 other animals received a double injection of ^{11}C-raclopride to assess test–retest reproducibility (see below). Each animal was positioned prone on the microPET bed, centering the brain in the FOV. The rat head was supported and secured to the bed to approximate a flat-skull orientation (*19*) in the camera FOV. Fully 3-dimensional listmode data were collected for 60 min using an energy window of 250–750 keV and a time window of 10 ns (default settings recommended by the manufacturer). MicroPET data acquisition was started simultaneously with ^{11}C-raclopride injection. The range in dose of ^{11}C-raclopride injected for all studies was 6.11–18.54 MBq (165–501 μCi). The specific activity at the time of injection varied from a minimum of 4.07 GBq/μmol (0.11 Ci/μmol) to a maximum of 48.1 GBq/μmol (1.3 Ci/μmol). This corresponded to a range of injected raclopride mass of 0.5–15 nmol/kg. For maximum sensitivity, coincidence data were binned into 3-dimensional sinograms using the full axial acceptance angle of the scanner. To preserve axial resolution, high sampling of the polar angle was used (21 segments). The binning produced 24 time frames (6 × 10 s, 3 × 20 s, 8 × 60 s, 4 × 300 s, and 3 × 600 s) and included subtraction of random coincidences collected in a delayed time window. The resulting sinograms were then rebinned using Fourier rebinning and reconstructed with 2-dimensional filtered backprojection using a ramp filter with cutoff at Nyquist via software provided by the manufacturer. Image pixel size was 0.85 mm transaxially with a 1.21-mm slice thickness.

Test–Retest Experiments

In 3 animals, injections of ^{11}C-raclopride were paired to address the reproducibility of microPET imaging in the same animal on the same day. In a fourth animal, raclopride (1 mg/kg) was coinjected with the second injection of ^{11}C-raclopride. The time between ^{11}C-raclopride injections varied from 2 to 4 h. Anesthesia was maintained during this time by intraperitoneal injection of ke-
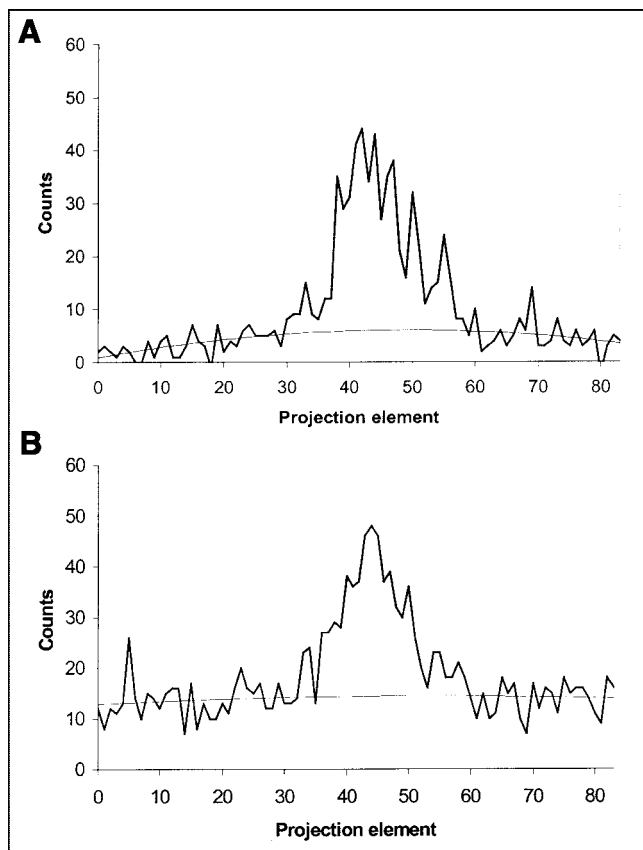
FIGURE 1. Typical sinogram projections in rat head with ^{11}C-raclopride. (A) Ten minutes after injection. (B) Sixty minutes after injection.

tamine/xylazine. The depth of anesthesia was monitored using respiration rate and whisker twitch.

Scatter Correction

For the scatter-corrected results, scattered events were subtracted from randoms-corrected sinograms based on a quadratic polynomial fit of projection data from outside the head in a manner similar to previously published tail-fitting methods (20,21). For improved statistics of the fit, radial projections from all azimuthal angles in the sinogram were summed. Thus, the same curve was subtracted from each projection within a given slice, although independent fits were made for each different slice. Because of the large transaxial FOV, it was possible to use conservative, fixed radial limits for the fit that excluded all possible true coincidences. Scatter-corrected sinograms were then subjected to the reconstruction methods described above. Note that this approach has the advantages of accounting for scatter from outside the FOV as well as any other potential sources of uniform background in the data.

Image Analysis

Region-of-interest (ROI) analysis was performed using vendor software (ASI Pro 1.1; Concorde Microsystems) on reconstructed images with and without scatter correction for each study. A circular ROI with an area of 15 pixels was drawn on the left striatum and right striatum from a single microPET image plane. Typically the striatum was delineated on 4 different coronal planes. One of 2 center planes was chosen for ROI analysis to

minimize axial partial-volume effects. A 29-pixel elliptic ROI was drawn on the cerebellum from a single coronal plane. The ROI for the cerebellum was typically 9 planes caudal to the striatum, corresponding to a distance of ~11 mm.

The harderian glands were used as anatomic landmarks to confirm identification of the correct plane for the striatum. The ROI for the striatum was most often located on the fifth coronal plane caudal to the last plane containing the harderian glands. This internal landmark was particularly useful for confirming proper ROI placement in low-contrast (low specific activity) studies. Left and right striatum data were averaged to give a single time–activity curve for the striatum. The DVR was computed from time–activity curves obtained from ROI analysis of both scatter-corrected and uncorrected images using the graphical analysis method without blood sampling (22).

RESULTS

Effects of Scatter Correction

The average scatter fractions of 3 representative sinogram projections (segment 0, plane 32 at 3, 10, and 60 min after injection) from 6 studies were determined to examine the effect of scatter as a function of time after injection of ^{11}C-raclopride. Total scatter fractions (ratio of scattered counts to trues-plus-scatter within the entire FOV) were 41% ± 6.6%, 41% ± 6.8%, and 64% ± 7.4% for 3, 10, and 60 min after injection, respectively. Scatter fractions within the rat head only were 24% ± 5.3%, 25% ± 5.7%, and 42% ± 7.6% for the same time frames. In both cases, the scatter fraction at 60 min is larger than at earlier time points. Two of the randoms-corrected sinogram projections from segment 0 (direct planes) in the center of the FOV (plane 32) are depicted in Figure 1. The smooth line represents the second-order polynomial fit of the background outside the object. For rat brain studies, sinogram counts from projection elements 0–24 and 60–83 were used in the fit. Figure

TABLE 1
Effect of Scatter Correction on Image ROI Data

Study	Δ (%) ROI	
	Striatum*	Cerebellum*
ptvec4	−4.7	−21
darat9	−3.0	−7.9
darat8	−5.5	−15
darat7	−4.3	−10
darat6	−4.9	−16
darat5	−2.7	−11
darat4	−2.6	−11
darat3	−3.2	−15
darat2†	−10†	−12†
darat1	−5.4	−10
daptvec2	−2.9	−17

*Sixty minutes after radiotracer injection.
†Blocking study: ^{11}C-raclopride coinjected with raclopride (1 mg/kg).
$\Delta = (ROI_{corrected} - ROI_{raw})/ROI_{raw} \times 100$.

TABLE 2
Effect of Scatter Correction on DVR

Study	DVR	DVR_{sc}*	% change[†]
daptvec2	2.31	2.55	+10
ptvec4	2.39	2.52	+5.4
darat1	1.62	1.65	+1.9
darat2	1.20	1.23	+2.5
darat3	2.08	2.08	0
darat4	1.90	1.97	+3.7
darat5	2.38	2.46	+3.4
darat6	2.56	2.62	+2.3
darat7	2.19	2.27	+3.7
darat8	2.29	2.35	+2.6
darat9	2.14	2.20	+2.8

*DVR after scatter correction.
[†]$(DVR_{sc} - DVR)/DVR \times 100$.

1 clearly shows the relative increase in sinogram background that is removed by the scatter correction.

The ROI analysis of scatter-corrected and uncorrected images is summarized in Table 1. The average change of the mean pixel values for the striatum and cerebellum after scatter correction was $-3.9\% \pm 1.9\%$ and $-13\% \pm 3.9\%$, respectively. The maximum change in the striatum was approximately -5%, whereas in 1 study the average pixel value in the cerebellum ROI decreased $>20\%$ after scatter correction. The average ($n = 9$) ST/CB ratio at 60 min increased $\sim 11\%$ from 3.36 to 3.74 after scatter correction. Study darat2 was excluded from the ratio computation because it was a blocking study with 1 mg/kg raclopride.

Study darat1 was also excluded because of low specific activity (15 nmol/kg).

Table 2 summarizes the effect of scatter correction on the DVR. The average change in the DVR after scatter correction was $+3.5\%$ (range, 0%–10%).
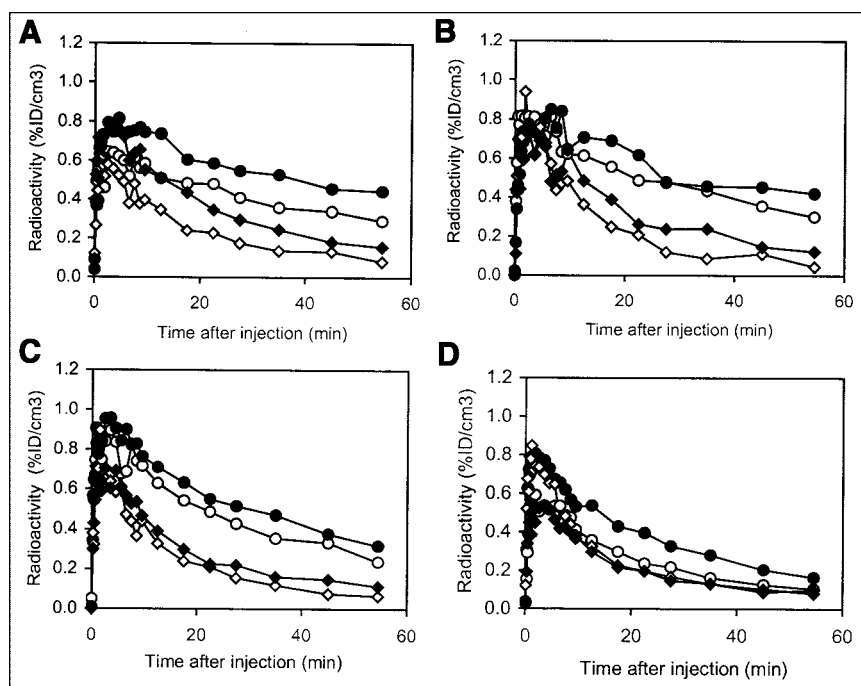
Reproducibility of ^{11}C-Raclopride Binding and DVR

Both the test–retest reproducibility of the DVR and the intersubject variability of the DVR were determined. Figure 2 presents ROI data from the 4 test–retest experiments, including the blocking study. The change in DVR (($DVR_2 - DVR_1$)/DVR_1) for the 3 test–retest experiments with scatter correction was -5.3%, -13%, and -6.4% (mean, $-8.3\% \pm 4.4\%$). Changes in the DVR using data uncorrected for scatter were slightly higher: -8.7%, -14%, and -6.6% (mean, $-9.9\% \pm 4.1\%$). To address intersubject variability, data from the single-injection studies were combined with data from the first injection of the test–retest experiments to give an average time–activity curve from 6 different rats as shown in Figure 3. Using the data from Figure 3, the average (from 1 to 60 min) coefficient of variation (CV) for the striatum and cerebellum was calculated to be 18% and 22%, respectively. The average DVR computed from the individual time–activity curves from the same 6 rats was 2.43 ± 0.19. The DVR for the blocking study was 1.23.

Effects of Tracer Specific Activity on DVR

Hume et al. (16) have determined the in vivo concentration of raclopride at which 50% of the available D2R is occupied (ED_{50}) in adult Sprague–Dawley rats using PET and ^{11}C-raclopride to be 17.1 nmol/kg. Using this number, receptor occupancy (Occ) can be calculated using the ex-

FIGURE 2. Test–retest experiments in rat brain with ^{11}C-raclopride. For all graphs, circles represent striatum and diamonds represent cerebellum. %ID/cm3 = percentage of injected dose per cubic centimeter. ● and ◆, First injection; ○ and ◇, Second injection. (A) First injection, 12.84 MBq (347 μCi; 3.8 nmol/kg raclopride); second injection, 11.91 MBq (322 μCi; 1.9 nmol/kg raclopride). (B) First injection, 7.22 MBq (195 μCi; 1.2 nmol/kg raclopride); second injection, 6.51 MBq (176 μCi; 1.0 nmol/kg raclopride). (C) First injection, 5.99 MBq (162 μCi; 0.5 nmol/kg raclopride); second injection, 13.88 MBq (375 μCi; 1.7 nmol/kg raclopride). (D) Blocking study: first injection, 17.58 MBq (475 μCi; 15 nmol/kg raclopride); second injection, 18.54 MBq (501 μCi; 1 mg/kg or 2,881 nmol/kg raclopride).
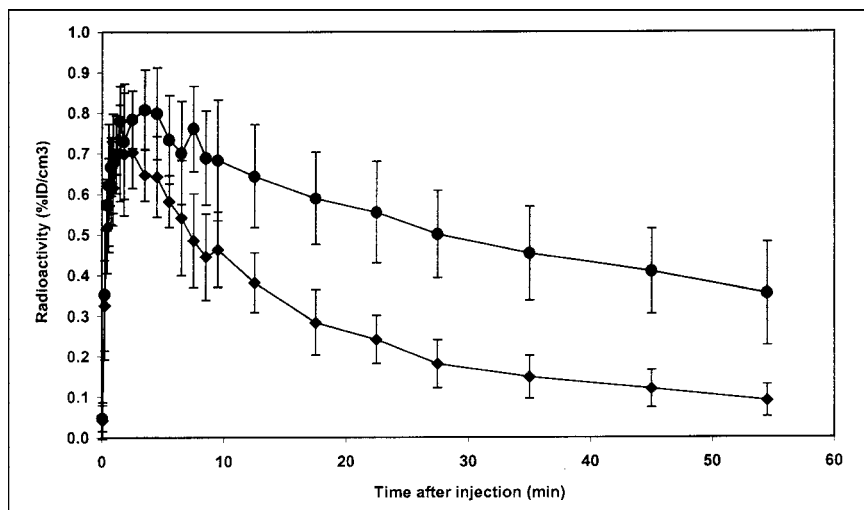
FIGURE 3. Reproducibility of ^{11}C-raclopride binding in brains of 6 adult rats. ●, Mean ROI value in striatum in 6 rats. ♦, Mean ROI value in cerebellum of 6 rats. Error bars are ±1 SD of mean. %ID/cm3 = percentage of injected dose per cubic centimeter.

pression Occ = L/(ED$_{50}$ + L), where L is the ligand (raclopride) dose in nmol/kg (23). Figure 4 shows the relationship between receptor occupancy calculated in this manner with the DVR determined with the microPET R4 from this work. In Figure 4, only studies darat1 through darat9 were included. These studies span 2 mo of operation in which isotope production and radiochemical synthesis (HPLC) conditions were unchanged, thus leading to a consistent determination of specific activity, ranging from 2.59 to 28.49 GBq/μmol (0.07–0.77 Ci/μmol) at the time of injection. Figure 4 clearly shows a dependence of the PET-determined DVR on the amount of raclopride mass injected. The studies tend to group with maximal specific activity (minimal occupancy) showing the highest DVR. In fact, the highest 4 DVRs correspond to the lowest 4 occupancies. For

each of these 4 studies, the unlabeled raclopride dose (expressed in nmol/kg rat weight) associated with the tracer radioactivity was <1.5 nmol/kg. The occupancy for each study in this group (Fig. 4) was <9%, and the average DVR for these studies was 2.43 ± 0.15. The next 3 highest DVRs correspond to a range of occupancy of 9%–18%. The average DVR for this lower specific activity group was 2.08 ± 0.11. The mass of raclopride injected for this group ranged from 1.6 to 3.7 nmol/kg. The mean DVRs of the 2 groups were statistically different using the Student t test ($P <$ 0.05).

The blocking study is included to demonstrate the dynamic range, or specific binding window, of the DVR.

DISCUSSION

Before the role of commercial animal PET cameras in biomedical research can be fully characterized, researchers must assess the quantitative capabilities of these new machines. For example, although all coincidence data in this study were corrected for both randoms contamination and detector dead-time losses, practical corrections for photon attenuation and scatter were not yet available from the microPET manufacturer at the time of these studies. Therefore, it is important to consider the impact of both of these corrections on microPET measures and, more specifically for this work, microPET determinations of the DVR. Although the absolute attenuation of deep rat brain regions can be significant (approaching 20%), the relative variation across the rat head is more likely to be closer to 10% because all parts of the image are attenuated to some extent. The average bias due to attenuation is accounted for by calibrating the camera with a phantom similar in size to the rat head (~3 cm in diameter). Furthermore, image attenuation corrections determined previously for the striatum and cerebellum in adult Sprague–Dawley rats using a custom-built animal PET camera (17) were found to be the same (16%). Because the data analysis methods used here (ST/CB
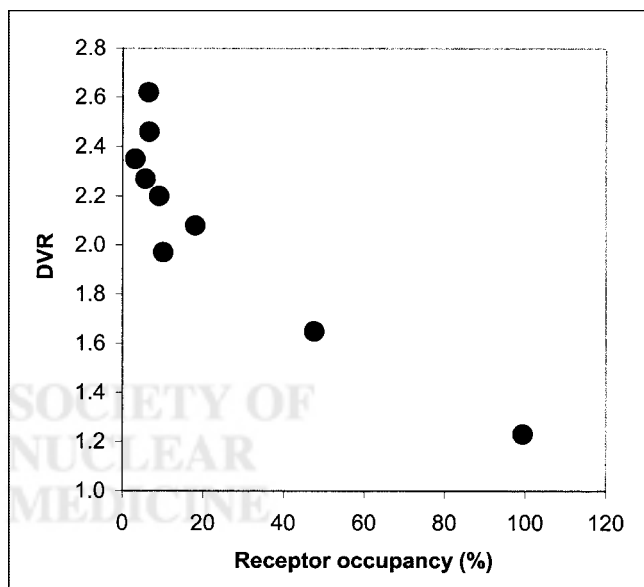

FIGURE 4. Effect of raclopride mass on DVR. Receptor occupancy is calculated from injected raclopride mass associated with tracer ^{11}C-raclopride according to Hume et al. (23).

and DVR) rely on the comparison (ratio) of a D2R-rich region (striatum) with a region used to estimate nonspecific binding (cerebellum), a constant attenuation correction factor for the striatum and cerebellum can be ignored. Scatter, on the other hand, manifests itself more as an image offset and, thus, can potentially have a much larger effect, particularly for low-activity reference regions such as the cerebellum.

No estimates of the background from photon scatter and its impact on the determination of ST/CB and DVR using the microPET R4 with ^{11}C-raclopride were available. With a diameter ($\sim$3 cm) that is small compared with the mean free path of a 511-keV photon in tissue ($\sim$10 cm), the adult rat head was expected to give microPET data with relatively small scatter fractions. However, the lack of septa in the microPET and its large axial FOV increase the probability that sinogram scatter fractions might be appreciable, especially because of activity outside the FOV. Indeed, our typical measured scatter fractions of 41% in early time frames are larger than those from the Concorde P4 primate scanner (32% for a 5-cm-diameter "rat" phantom (1)), which is consistent with an axial acceptance angle almost double that of the P4. The tail-fitting scatter correction algorithm produced a small but consistent effect on the DVR, increasing the DVR an average of 3.5% with a maximum of 10%. ROI data showed a more significant effect, especially when derived from brain regions of lower accumulation of tracer radioactivity such as the cerebellum, where mean ROI pixel values from scatter-corrected images decreased as much as 20% compared with uncorrected image data.

An interesting observation is the significant increase in sinogram background from the beginning of the study to the end. If related to scatter, it is presumably caused by a redistribution of radioactivity from inside to outside the FOV. At the low activity levels near the end of a scan, other low-level sources of uniform background might also contribute, such as an imperfect randoms correction or the natural radioactivity of lutetium oxyorthosilicate (LSO). A full explanation of this effect is under investigation but, regardless of the cause, it is significant and demonstrates the need to incorporate a background subtraction technique into the recommended configuration of the microPET R4 to obtain accurate tracer kinetic information.

Because at least 1 dimension of a brain structure (e.g., striatum) studied in this work is near ($\sim$2 $\times$ FWHM) the spatial resolution of the scanner, measurements of radioactivity concentration in this region will be underestimated due to the partial-volume effect (24). An appreciation of the magnitude of partial-volume errors can be gleaned from comparisons with ex vivo measurements. For example, the ST/CB of $\sim$4 determined at 60 min after ^{11}C-raclopride injection can be compared with ex vivo data—dissected brain regions counted in a well counter—giving ratios of $\sim$9 (7). This partial-volume error in ST/CB can be attributed primarily to errors in striatal ROI values because the

cerebellum, a brain region of nonspecific ^{11}C-raclopride binding, is surrounded by tissue of similar uptake, thereby masking the effect of spillover activity from surrounding tissue. The effects of partial volume on the ST/CB can also be observed when comparing data from PET scanners of different spatial resolutions. For example, the measurement of higher ST/CB ratios in this study ($\sim$4) compared with values reported by Hume et al. (7) ($\sim$2.5) is consistent with an improved radioactivity recovery that can be expected with the higher spatial resolution of the microPET R4 ($\sim$2 mm), given similar ROI sizes.

Contamination of radioactivity from one region to a nearby region (spillover) due to the partial-volume effect will also give rise to errors in ROI radioactivity concentration determinations. Spillover errors in rat brain imaging can be of special concern because of the existence of 2 discrete extracerebral structures just anterior to the brain. These structures, the harderian glands, often exhibit high radioactivity uptake that can result in significant spillover errors in nearby brain regions, such as the prefrontal cortex (25). With the advent of new high-resolution animal cameras such as the microPET R4, this problem has diminished (14,26–28). For example, Nikolaus et al. (14), using the specific D2R ligand ^{18}F-N-methyl-benperidol and a high-resolution PET camera ($\sim$2.1-mm FWHM), determined the spillover error in the striatum from harderian gland uptake to be $\sim$5%.

The magnitude of the spillover errors to the striatum is not just a function of the distance between structures relative to the camera resolution but also depends on the relative uptake in the 2 regions and, therefore, must be determined for each tracer. Meyers et al. (17) and Lammertsma et al. (29) have determined the spillover fraction from the harderian glands to the striatum for ^{11}C-raclopride in a rat imaged with a clinical human camera (FWHM = 5.5 mm) to be 0%–3.5% in control binding experiments. The higher resolution of the microPET R4 reduces this fraction below 3.5% and, therefore, this effect should be negligible in our studies.

A primary goal of this work was to measure the test–retest reproducibility of ^{11}C-raclopride binding in the rat brain as reflected in changes in the DVR. The average change in the DVR of $\sim$8% observed in this work is similar to the reproducibility obtained in humans (30) and baboons (31) and, therefore, suggests that microPET imaging can be successfully used to study the D2R system in the rat brain. However, the large variability of the test–retest change, including the observation of a −13% change in the second paired control study, suggests that determinations of the DVR in rat brain may be more sensitive to PET experimental conditions than primate imaging performed using a standard clinical camera. Although increased noise from the use of a low injected dose ($\sim$6.85 MBq [$\sim$185 μCi]) may be contributing to the larger test–retest error in the second paired study (Fig. 2B), the observation that all 3 retest

studies gave a lower DVR value suggests that there may be a bias in the retest experiment.

Potential PET experimental conditions creating a bias in the retest data include tracer-specific activity and anesthesia. Two of the 3 retest experiments, including the study giving the largest DVR change, had a lower raclopride mass administered to the animal, so a consistently smaller retest DVR cannot be explained by specific activity differences. The other important experimental condition that is significantly different from PET studies with primates is the method of anesthesia used in this work. The average dose of ketamine (intraperitoneal) used in this study was 85 mg/kg/h. Tsukada et al. (32) have shown that ketamine can reduce raclopride binding in the primate brain in a dose-dependent manner for 3–10 mg/kg/h given intravenously. The lower retest DVR observed in this work is consistent with the fact that retest experiments are performed (2–4 h later) after a larger ketamine dose has been administered to the animal and, therefore, may show a larger decrease in ^{11}C-raclopride binding.

The reproducibility of the DVR of ^{11}C-raclopride measured in 6 different rats is similar to data reported by Myers et al. (17) for a similar range of specific activity. These authors determined the binding potential (DVR-1) in 15 rats to be 0.79 ± 0.09 (coefficient of variation [CV] = 11%) using a small-animal PET camera (20). In this study, the average DVR for 6 rats was 2.43 ± 0.19 (CV = 8%). This gives an average binding potential of 1.43 ± 0.19 (CV = 13%). The variability of the binding potential measured here is similar to published data even with a relatively small sample size.

The average binding potential of 1.43 determined is almost 2 times the binding potential reported by Hume et al. (7). Assuming similar ROI sizes, this is consistent with an improved radioactivity recovery in the striatum due to a decrease in the partial-volume error associated with the higher resolution of the microPET R4. The dynamic range, or specific binding window, also increased by at least a factor of 2 in this work because blocking studies gave similar binding potentials. Even if a smaller ROI size (resulting in improved radioactivity recovery) underlies the determination of a higher binding potential in this work, the fact remains that reproducible data were obtained with ~30-pixel ROIs, giving a robust change in binding potential (~0.2–1.4). This result confirms that the microPET R4 has both sufficient sensitivity and resolution to perform experiments of the D2R system in the rat brain using the DVR.

Much attention has been given to the issue of tracer-specific activity and the limits it puts on high-resolution PET imaging of small laboratory animals, particularly in mice (11,23,33). It has been suggested that a receptor occupancy of 1% is required to satisfy tracer kinetic modeling (23,34). Morris and London (35) have simulated studies with primates and have concluded that a dose of raclopride of 0.5 nmol/kg was required before the binding potential was compromised. This dose corresponds to a receptor occupancy of 3% using the analysis of Hume et al. (23). Although a rigorous saturation study was not performed in this work, the specific activity of ^{11}C-raclopride used varied by an order of magnitude. Figure 4 clearly shows an effect of specific activity (raclopride mass) on the measured DVR. From these data and a simple grouping of studies using a mesh of 9% occupancy, a minimum threshold for raclopride mass can be obtained. Under the present experimental conditions, this threshold is <1.5 nmol/kg raclopride. The mean DVR ($n = 4$) obtained with raclopride doses <1.5 nmol/kg was significantly different ($P < 0.05$) than that obtained from studies in the range of 1.5–3.7 nmol/kg ($n = 3$). Furthermore, within the high specific activity group (<1.5 nmol/kg) there was no correlation between raclopride mass and DVR. Previous work has demonstrated a significant change in experimentally determined binding potential in a rat when raclopride mass is in the range of 1 nmol/kg (13) to 5 nmol/kg (17).

Although this threshold does not address the issue of pharmacologic response and receptor occupancy, it does establish a guideline for microPET R4 rat brain experiments given the experimental conditions of anesthesia, camera performance, and ^{11}C-raclopride specific activity used in these investigations. Extension of these findings to possible microPET R4 determinations of the DVR in the mouse brain, however, must be made cautiously. In fact, recent results in our laboratory have shown that, although it was possible to observe differences in both DVR and ST/CB between groups of wild-type and D2 knockout mice using the microPET R4, the average D2R occupancy in the mouse brain was estimated to be ~50% (11). Therefore, further investigations must be performed before the usefulness of microPET R4 imaging of D2R function in the mouse brain with ^{11}C-raclopride can be established.

CONCLUSION

The commercial microPET R4 and its associated software can be used for dynamic measurements of localized ^{11}C-raclopride radioactivity in a rat brain such that ROI analysis using the DVR can be used as a specific and reproducible measure of D2R availability. Its intrinsic spatial resolution of <2 mm provides improved recovery of radioactivity compared with first-generation small-animal cameras. The microPET R4, with its 4 rings of LSO block detectors covering a large solid angle, demonstrated an absolute sensitivity that did not put any significant constraints on the use of readily available ^{11}C-raclopride specific activity and afforded reproducible DVR measures with <925 MBq (<250 μCi) in adult Sprague–Dawley rats.

Custom scatter correction software based on fitting of data outside the object was easy to implement and improved specific measures of D2R availability, including the ST/CB ratio and DVR, although the average improvement in the DVR was small (~3.5%). Overall test–retest reproducibility of the scatter-corrected data (average = −8%) is similar to

results obtained in baboons and humans using clinical PET and, therefore, should be sufficient for many types of drug challenge studies. Reduced variability is expected using larger sample sizes, although more studies may be needed to assess the contribution of the possible interaction of ketamine anesthesia with dopaminergic function (*32*) on test–retest reproducibility.

A threshold for raclopride mass below which a change in the DVR could not be measured was determined experimentally to be ~1.5 nmol/kg. This threshold provides a useful guideline for carrying out microPET R4 experiments under the specific experimental conditions of anesthesia, camera performance, and ^{11}C-raclopride specific activity described in this work and is similar to results obtained using other small-animal PET cameras (*13*).

ACKNOWLEDGMENTS

REFERENCES

1. Tai YC, Chatziioannou A, Siegel S, et al. Performance evaluation of the micro-PET P4: a PET system dedicated to animal imaging. *Phys Med Biol.* 2001;46:1845–1862.
2. Jeavons AP, Chandler RA, Dettmar CAR. A 3D HIDAC-PET camera with sub-millimetre resolution for imaging small animals. *IEEE Trans Nucl Sci.* 1999;46:468–473.
3. Hume SP, Jones T. Positron emission tomography (PET) methodology for small animals and its application in radiopharmaceutical preclinical investigation. *Nucl Med Biol.* 1998;25:729–732.
4. Burns HD, Hamill TG, Eng W, Francis B, Fioravanti C, Gibson RE. Positron emission tomography neuroreceptor imaging as a tool in drug discovery, research and development. *Curr Opin Chem Biol.* 1999;3:388–394.
5. Hume SP, Myers R. Dedicated small animal scanners: a new tool for drug development? *Curr Pharm Des.* 2002;8:1497–1511.
6. Chatziioannou AF. Molecular imaging of small animals with dedicated PET tomographs. *Eur J Nucl Med.* 2002;29:98–114.
7. Hume SP, Lammertsma AA, Myers R, et al. The potential of high-resolution positron emission tomography to monitor striatal dopaminergic function in rat models of disease. *J Neurosci Methods.* 1996;67:103–112.
8. Ishiwata K, Ogi N, Hayakawa N, et al. Positron emission tomography and ex vivo and in vitro autoradiography studies on dopamine D2-like receptor degeneration in the quinolinic acid-lesioned rat striatum: comparison of [^{11}C]raclopride, [^{11}C]nemonapride and [^{11}C]*N*-methylspiperone. *Nucl Med Biol.* 2002;29:307–316.
9. Araujo DM, Cherry SR, Tatsukawa KJ, Toyokouni T, Kornblum HI. Deficits in striatal dopamine D_2 receptors and energy metabolism detected by in vivo micropet imaging in a rat model of Huntington's disease. *Exp Neurol.* 2000;166:287–297.
10. Tsukada H, Kreuter J, Maggos CE, et al. Effects of binge pattern cocaine administration on dopamine D_1 and D_2 receptors in the rat brain: an in vivo study using positron emission tomography. *J Neurosci.* 1996;16:7670–7677.
11. Thanos PK, Taintor NB, Alexoff DL, et al. In vivo comparative imaging of dopamine D2 knockout and wild-type mice with ^{11}C-raclopride and microPET. *J Nucl Med.* 2002;43:1570–1577.
12. Budinger TF, Benaron DA, Koretsky AP. Imaging transgenic animals. *Annu Rev Biomed Eng.* 1999;1:611–648.
13. Opacka-Juffry J, Ashworth S, Ahier RG, Hume SP. Modulatory effects of L-DOPA on D2 dopamine receptors in rat striatum, measured using in vivo microdialysis and PET. *J Neural Transm.* 1998;105:349–364.
14. Nikolaus S, Larisch R, Beu M, Vosberg H, Muller-Gartner H-W. Imaging of striatal dopamine D_2 receptors with a PET system for small laboratory animals in comparison with storage phosphor autoradiography: a validation study with ^{18}F-(*N*-methyl)benperidol. *J Nucl Med.* 2001;42:1691–1696.
15. Umegaki H, Ishiwata K, Ogawa O, et al. In vivo assessment of adenoviral vector-mediated gene expression of dopamine D_2 receptors in the rat striatum by positron emission tomography. *Synapse.* 2002;43:195–200.
16. Hume SP, Opacka-Juffry J, Myers R, et al. Effect of L-dopa and 6-hydroxydopamine lesioning on [^{11}C]raclopride binding in rat striatum, quantified using PET. *Synapse.* 1995;21:45–53.
17. Meyers R, Hume SP, Ashworth S, et al. Quantification of dopamine receptors and transporter in rat striatum using a small animal PET scanner. In: Meyers R, Cunningham V, Bailey D, Jones T, eds. *Quantification of Brain Function Using PET.* London, U.K.: Academic Press, Inc.; 1996:12–15.
18. Farde L, Hall H, Ehrin E, Sedvall G. Quantitative analysis of D2 dopamine receptor binding in the living human brain by PET. *Science.* 1986;231:258–261.
19. Paxinos G, Watson C. *The Rat Brain in Stereotaxic Coorindates.* 2nd ed. London, U.K.: Academic Press; 1986:8–15.
20. Bloomfield PM, Myers R, Hume SP, Spinks TJ, Lammertsma AA, Jones T. Three-dimensional performance of a small-diameter positron emission tomograph. *Phy Med Biol.* 1997;42:389–400.
21. Cherry SR, Huang S-C. Effects of scatter on model parameters in 3D PET studies of the human brain. *IEEE Trans Nucl Sci.* 1995;42:1174–1179.
22. Logan J, Fowler JS, Volkow ND, et al. Distribution volume ratios without blood sampling from graphical analysis of PET data. *J Cereb Blood Flow Metab.* 1996;16:834–840.
23. Hume SP, Gunn RN, Jones T. Pharmacological constraints associated with positron emission tomographic scanning of small laboratory animals. *Eur J Nucl Med.* 1998;25:173–176.
24. Hoffman EJ, Phelps ME. Positron emission tomography: principles and quantitation. In: Phelps ME, Mazziotta JC, Schelbert HR, eds. *Positron Emission Tomography and Autoradiography Principles and Applications for the Brain and Heart.* New York, NY: Raven Press; 1986:237–286.
25. Kuge Y, Minemastsu K, Hasegawa Y, et al. Positron emission tomography for quantitative determination of glucose metabolism in normal and ischemic brains in rats: an insoluble problem by the harderian glands. *J Cereb Blood Flow Metab.* 1997;17:116–120.
26. Moore AH, Osteen CL, Chatziioannou AF, Hovda DA, Cherry SR. Quantitative assessment of longitudinal metabolic changes in vivo after traumatic brain injury in the adult rat using FDG-microPET. *J Cereb Blood Flow Metab.* 2000;20:1492–1501.
27. Fukuyama H, Hayashi T, Katsumi Y, Tsukada H, Shibasaki H. Issues in measuring glucose metabolism of rat brain using PET: the effect of harderian glands on the frontal lobe. *Neurosci Lett.* 1998;255:99–102.
28. Kornblum HI, Araujo DM, Annala AJ, Tatsukawa KJ, Phelps ME, Cherry SR. In vivo imaging of neuronal activation and plasticity in the rat brain by high resolution positron emission tomography (microPET). *Nature Biotech.* 2000;18:655–660.
29. Lammertsma AA, Hume SP, Myers R, Bloomfield PM, Rajeswaran S, Jones T. RAT-PET: a bridge between ex vivo animal and in vivo patient studies. In: Uemura K, Lassen NA, Jones T, Kanno I, eds. *Quantification of Brain Function: Tracer Kinetics And Image Analysis in Brain PET. Proceedings of Brain PET '93, Akita, Japan, May 29–31, 1993.* International Congress Series 1030. Tokyo, Japan: Elsevier Science Publishers; 1993:321–329.
30. Volkow ND, Fowler JS, Wang G-J, et al. Reproducibility of repeated measures of carbon-11-raclopride binding in the human brain. *J Nucl Med.* 1993;34:609–613.
31. Dewey SL, Smith GS, Logan J, et al. GABAergic inhibition of endogenous dopamine release measured in vivo with ^{11}C-raclopride and positron emission tomography. *J Neurosci.* 1992;12:3773–3780.
32. Tsukada H, Harada N, Nishiyama S, et al. Ketamine decreased striatal [^{11}C]raclopride binding with no alterations in static dopamine concentrations in the striatal extracelluar fluid in the monkey brain: multiparametric PET studies combined with microdialysis analysis. *Synapse.* 2000;37:95–103.
33. Meikle SR, Eberl S, Fulton RR, Kassiou M, Fulham MJ. The influence of tomograph sensitivity on kinetic parameter estimation in positron emission tomography imaging studies of the rat brain. *Nucl Med Biol.* 2000;27:617–625.
34. Huang S-C, Phelps ME. Principles of tracer kinetic modeling in positron emission tomography and autoradiography. In: Phelps ME, Mazziotta JC, Schelbert HR, eds. *Positron Emission Tomography and Autoradiography Principles and Applications for the Brain and Heart.* New York, NY: Raven Press; 1986:287–346.
35. Morris ED, London ED. Limitations of binding potentials as a "clinical" measure of receptor function: susceptibility to mass. [abstract]. *Neuroimage.* 1997;5:B61.